processes

MDPI

Article

Evaluating Nitrogen Gas Injection Performance for Enhanced Oil Recovery in Fractured Basement Complex Reservoirs: Experiments and Modeling Approaches

Ying Jia [1,2], Jingqi Ouyang [1,2], Feng Xu [1,2,3,*], Xiaocheng Gao [4], Juntao Zhang [1,2], Shiliang Liu [5] and Da Li [5]

[1] CNPC International (Chad) Co., Ltd., N'Djamena BP 2519, Chad
[2] China National Oil and Gas Exploration and Development Company Ltd., Beijing 100034, China
[3] Research Institute of Petroleum Exploration & Development, Co., Ltd., CNPC, Beijing 100085, China
[4] PetroChina Huabei Oilfield Company, Renqiu 062552, China
[5] Research Institute of Exploration and Development, PetroChina Yumen Oilfield Company, Jiuquan 735019, China
* Correspondence: jack_xf@126.com

Abstract: This study explored the effectiveness of gas injection for enhanced oil recovery (EOR) in fractured basement complex reservoirs, combining laboratory experiments with numerical simulation analyses. The experiments simulated typical field conditions, focusing on understanding the interaction between the injected gas and the reservoir's fracture–matrix system. The laboratory results showed that under the current reservoir pressure and temperature conditions, nitrogen gas flooding in the fractured matrix achieved a superior oil recovery efficiency compared to that of the other gases tested (CO_2, APG, and oxygen-reduced air), exhibiting the most favorable movable oil saturation range and the lowest residual oil saturation. To evaluate the performance of nitrogen gas injection in a fractured basement complex reservoir, a 3D reservoir model with complex natural fractures was built in a numerical reservoir simulator. Special methods were required for the geological modeling and reservoir simulation, with the specific principles outlined. Numerical simulations of gas injection into fractured basement complex reservoirs revealed that cyclic gas injection was identified as the most effective strategy, balancing incremental oil recovery with minimized gas channeling risks. This study demonstrated that the optimal injection location and rate are crucial factors affecting the recovery performance. These findings provided actionable insights for implementing gas injection EOR strategies in fractured basement complex reservoirs, highlighting the importance of optimizing the injection parameters to maximize the recovery.

Keywords: basement complex; granite reservoir; gas injection; natural fractures; depletion development

Academic Editors: Qingbang Meng and Yidong Cai

Received: 23 November 2024
Revised: 30 December 2024
Accepted: 20 January 2025
Published: 24 January 2025

Citation: Jia, Y.; Ouyang, J.; Xu, F.; Gao, X.; Zhang, J.; Liu, S.; Li, D. Evaluating Nitrogen Gas Injection Performance for Enhanced Oil Recovery in Fractured Basement Complex Reservoirs: Experiments and Modeling Approaches. *Processes* **2025**, *13*, 326. https://doi.org/10.3390/pr13020326

1. Introduction

The study of basement complex oil reservoirs has garnered significant attention in the oil and gas industry over several decades. Early research efforts focused on understanding the characteristics of these reservoirs in the United States, with investigations into their nature and production potential [1–5]. In South Vietnam, Kireev et al. explored the composition, structure, and oil-bearing potential of the basement complex in the White Tiger Field, a hallmark example of fractured basement reservoirs [6]. Similarly, Malim et al. examined the challenges and outcomes of formation evaluation in a fractured basement reservoir in Malaysia, emphasizing the intricacies of assessing such geologically complex

systems [7]. More recently, McGeer et al. characterized a highly complex fractured basement reservoir in Yemen, detailing the interactions between the production mechanisms in the fractured basement and the overlying sandstone reservoir [8]. These studies collectively highlighted the global diversity of fractured basement reservoirs and underscored the importance of understanding their unique characteristics to optimize recovery strategies.

Fractured basement reservoirs present significant challenges due to their pronounced static and dynamic heterogeneity, which stem from the intricate distribution of the fractures and complex matrix interactions [9]. To maintain the reservoir pressure in such systems, water and gas injection have frequently been employed. However, the presence of fractures has often led to rapid water channeling, which can bypass substantial portions of the oil, leaving it trapped within the reservoir matrix. To address these challenges, various gas injection techniques, including miscible and immiscible methods, have been investigated as effective means to enhance the oil recovery in fractured basement reservoirs [10]. Research indicates that gas injection can significantly improve the recovery factor by increasing the interaction between the injected gas and trapped hydrocarbons, thereby enhancing the oil displacement [11]. Gas flooding, in particular, offers the advantage of penetrating microscopic fractures and pores, improving the sweep efficiency and mobilizing oil that would otherwise remain inaccessible. Moreover, gas injection leverages the gravity difference between the oil and gas by introducing gas at the upper sections of the reservoir, facilitating oil recovery from the middle and lower zones of the fractured basement complex. This gravity-assisted mechanism not only improves the displacement efficiency but also maximizes the utilization of the reservoir's natural characteristics to enhance the overall recovery [12–26].

These heterogeneities significantly influence the fluid flow behavior, complicating the processes of characterization, modeling, and simulation [27–36]. To address these complexities, researchers have developed two primary modeling approaches to understanding the fluid dynamics in fractured systems better: dual-porosity (dual-continuum) models and discrete fracture models (DFMs) [37–41]. These methodologies have offered unique strengths in tackling the intricate interactions within fractured reservoirs. Dual-porosity (dual-continuum) models are particularly well suited to large-scale reservoir simulations, as they efficiently approximate the impact of fractures that are too small to be explicitly resolved. However, these models struggle to accurately capture the highly heterogeneous distribution of the fracture properties, which can lead to oversimplified representations of the fluid flow dynamics. On the other hand, DFMs provide a more detailed and accurate depiction of the fluid flow in reservoirs with significant fracture heterogeneity. By explicitly modeling the individual fractures, DFMs effectively capture the dynamic interactions between the fractures and the matrix. Despite their accuracy, DFMs are computationally demanding, especially for large reservoirs with complex fracture networks. Additionally, they require high-resolution data on the fracture geometry and distribution, which is often challenging to obtain in practice. To model and simulate the interactions between the fractured basement and the overlying sandstone reservoir, special methods are required for geological modeling and reservoir simulation, with the specific principles outlined in this paper.

In this study, both laboratory experiments and reservoir simulations were carried out to evaluate the feasibility and benefits of gas injection into fractured basement complex oil reservoirs. Several key physical tests were conducted to understand the behavior of gas injection, including CO_2, associated petroleum gas (APG), air, and N_2. For the simulation, a 3D fractured basement complex model was constructed to simulate the performance of gas injection, optimize the gas injection strategies by simulating different injection scenarios,

and quantify the incremental recovery obtained from gas injection compared to that with other methods.

Unlike earlier studies that predominantly explored miscible gas injection techniques or emphasized geological characterization, this study provides a comprehensive analysis of nitrogen injection as an immiscible gas for enhanced oil recovery. Furthermore, our investigation develops and validates an optimized cyclic gas injection method tailored to the unique geological and fluid characteristics of fractured basement reservoirs. These contributions build on prior findings and offer practical insights for improving the recovery factors in similarly complex reservoir systems.

2. Methods

This study employs a multidisciplinary approach to evaluating the feasibility and optimization of nitrogen gas injection into fractured basement complex reservoirs. Laboratory experiments were conducted to measure key parameters, including the minimum miscibility pressure (MMP), the oil recovery efficiency through core flooding, and the oil–gas relative permeability in fractured and matrix samples. The numerical simulations utilized a sandstone model and a fractured basement reservoir model to simulate the fluid flow dynamics under various injection scenarios. The models were calibrated using production data through history matching to ensure their accuracy. A combination of geological characterization, experimental results, and numerical simulations enabled a comprehensive validation and provided insights into the optimal gas injection strategies. The flowchart is shown in Figure 1.

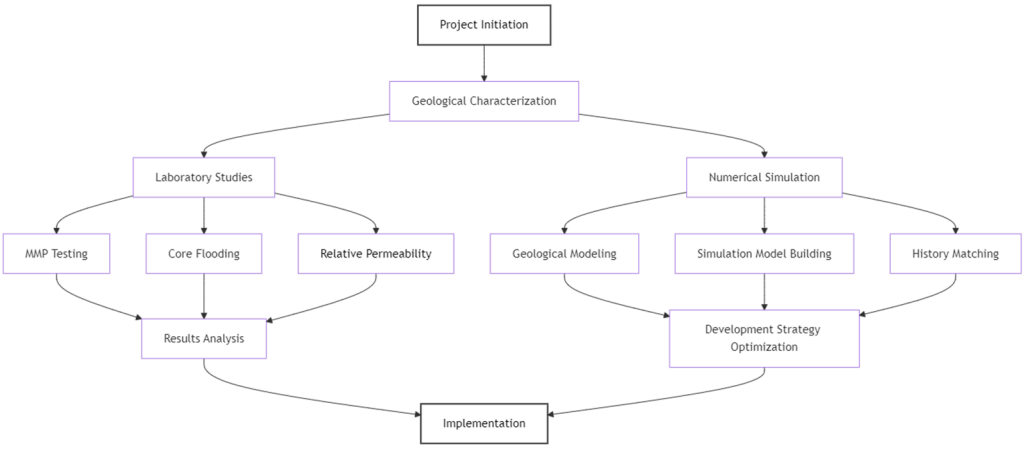

Figure 1. Comprehensive methodology flowchart of gas injection into fractured basement complex reservoirs.

2.1. Laboratory Methods

Laboratory experiments were conducted to evaluate the efficiency of nitrogen gas injection in enhancing the oil recovery within fractured reservoirs. The minimum miscibility pressure (MMP) was determined using a slim-tube apparatus under reservoir conditions (96.8 °C) for gases including N_2, CO_2, and associated petroleum gas (APG). Long-core flooding experiments were performed on fractured core samples to assess the oil recovery efficiency for each gas type, simulating immiscible displacement processes. Additionally, oil–gas relative permeability curves were measured for both matrix and fractured systems to capture the flow behavior and the saturation characteristics under various injection scenarios. These experiments provided critical input parameters for validating the numerical simulations and optimizing the gas injection strategies.

The oil sample used in the laboratory test was from a typical well in a fractured basement complex oil reservoir, which was a black oil system. The APG used in the

laboratory test came from a high-gas-rate well in the main oilfield, with 67.9% C_1 + N_2 and 32.1% C_2–C_6 + CO_2, indicating a rich gas with a high methane content, as shown in Table 1. The test conditions were the same in terms of formation temperature and pressure.

Table 1. Composition of the APG.

Component	Composition, mol%
CO_2	0.32
N_2	5.64
C_1	62.25
C_2	11.05
C_3	13.05
iC_4	3.63
nC_4	2.84
iC_5	0.41
nC_5	0.15
C_{6+}	0.67

2.1.1. The Minimum Miscibility Pressure (MMP) Test

The slim-tube experiment was the primary method for determining the minimum miscibility pressure (MMP) of a given injection gas. The slim-tube experiment was conducted following the standard procedures in the petroleum industry. The experimental temperature was set to match the reservoir temperature of the fractured basement complex reservoir. The injection pump operated in a constant-speed mode, with the displacement pressure controlled by the back pressure according to the designed value. The displacement rate was 0.2 mL/min, and the displacement process ended when the injected gas volume reached 1.2 PV. Detailed parameters for the slim-tube experiment are listed in Table 2.

Table 2. Parameters for the slim-tube experiment.

Diameter (mm)	Length (cm)	Pore Volume (mm^3)	Temperature (°C)	Highest Pressure (MPa)	Medium
1.05	20.0	73.5	96.8	25	quartz sand

2.1.2. Core Flooding Experiments

Gas flooding has received extensive attention due to its low cost and high effectiveness. This paper explored the differences in the oil recovery efficiency among four gases (CO_2, APG, oxygen-reduced air, and N_2) by comparing their flooding efficiencies in long-core experiments and examining the underlying reasons for these differences.

A long core with a length of 45.25 cm and a diameter of 2.48 cm was selected, with a porosity of 5.1% and a permeability of 62.13 mD. Light crude oil with a viscosity of 2.55 mPa·s was used, as shown in Table 3. There were 4 different displacement gases: CO_2, associated gas, air, and N_2. After saturating the core sample with water, it was saturated with crude oil to establish the initial oil saturation. We performed displacement experiments using CO_2, associated gas, air, and N_2, recording the pressure changes and oil production during the displacement process. We maintained a constant temperature throughout the experiment to simulate reservoir conditions.

Table 3. Core properties and conditions for core flooding experiments.

L cm	D cm	K_a mD	Φ %	μ_o mPa·s	S_o %
45.25	2.48	62.13	5.1	2.55	65.6

2.1.3. The Relative Permeability Experiment

To study the effectiveness in terms of the gas injection displacement efficiency in the fractured basement complex reservoir, a series of gas flooding experiments were conducted. A standard workflow for testing the relative permeability of two-phase fluids (oil and gas) in sandstone and fractured basement rock was used to measure the oil–gas relative permeability curve during gas flooding under unsteady conditions. In these tests, the oil's viscosity was 2.55 mPa·s, and water's viscosity was 0.019 mPa·s. The experimental data for oil–gas relative permeability and the corresponding permeability curves for each core during gas flooding were determined and normalized.

This study conducted four sets of relative permeability experiments on four core samples, aiming to explore the differences in the flow characteristics between the matrix cores and artificially fractured matrix cores under gas flooding conditions (Seen in Table 4).

Table 4. Statistics in terms of characteristic values of oil–gas relative permeability curves.

Sample No.	Type	L, cm	D, cm	Ka, mD	Ko, mD	Porosity, %	Swi, %	Sor, %	ED, %
2-8-3	Matrix	2.442	2.477	2.929	0.153	13.8	38.5	37.5	42.4
2-8-1	Matrix	4.338	2.481	0.559	0.022	8.6	42.0	40.5	32.3
1-3-1	Fracture + Matrix	6.638	2.48	62.4	13.1	4.6	35.1	30.1	52.12
2-9-2	Fracture + Matrix	4.086	2.483	59.6	11.6	4.8	35.8	29.4	53.32

2.2. Numerical Simulation Methods

2.2.1. Geological Modeling

The basement complex was an assemblage of metamorphic and igneous rocks underlying stratified rocks [42]. The research target was a triangular closed fault block bounded by faults that had developed in three directions: northeast, northwest, and southeast. It featured the structural characteristic of being higher in the northeast and lower in the southwest, with the highest point located in the northwest. The formation dip angle reached up to 30 degrees. The shale interlayers within the oil reservoir in the block were unevenly developed and directly overlaid the fractured granite, with unified oil–water contact. In Figure 2, the structural and lithological characteristics of the reservoir are illustrated. The colors represent different geological units and features: fractured granite, overlying sandstone, and fault zones. The unified oil–water contact (blue line) indicates a single-temperature–pressure system.

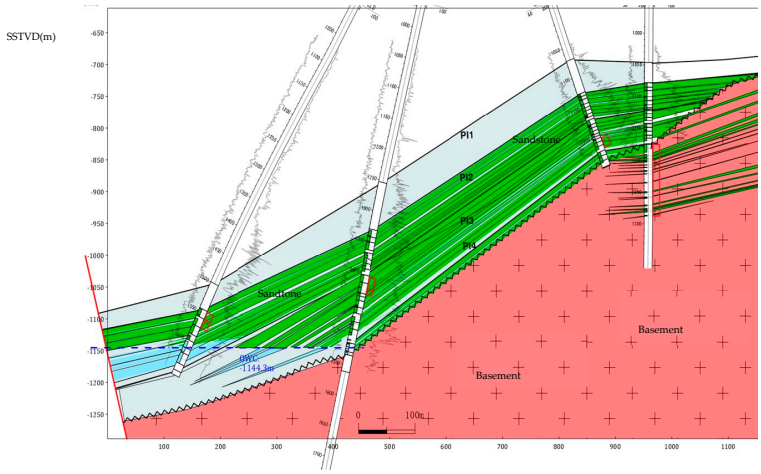

Figure 2. Cross-section of the fractured basement complex reservoir.

The reservoir's stratigraphy can be divided into two main units: the basement complex, primarily composed of granite, granodiorite, and granodioritic gneiss, and the overlying

sandstone, characterized by dark brown, gravel-bearing, medium to coarse sandstone. The sandstone was generally a medium-porosity, medium- to high-permeability oil reservoir, with an average porosity of 18.4% and an average permeability of 638 $\times$ 10^{-3}μm^2. DST (Drill Stem Test) data indicate that the temperature and pressure vs. depth curves of the field's sandstone and basement reservoirs were consistent, suggesting that the sandstone and the basement reservoirs form a single-temperature–pressure system. The crude oil in this block was light oil, with a density of 0.8429 to 0.8558 g/cm^3 at 20 °C and a gravity ranging from 33.25 to 35.80° API. The formation temperature of the fractured basement complex was 96.8 °C, the formation pressure was 12.3 MPa, and the gas/oil ratio was 15.9 m^3/m^3.

The reservoir is predominantly composed of fractured granite with overlying sandstone. The granite matrix has a low porosity and permeability, while the fractures act as the primary flow pathways, and the fractures on the top of the basement are more developed. The fractured granite reservoir spanned a large thickness, with a depth extending 190 m below the basement surface, while the main reservoir's thickness was mostly within 60 m. The good reservoir zones in the basement were distributed in a quasi-layered pattern, and generally, the reservoirs in the structural high were superior to those in the structural low. Affected by multiple phases of tectonic movements, the basement complex had well-developed faults, with two main sets of faults oriented in the NW and NE directions. Among these, the northwest-oriented faults were the primary ones. Based on the imaging logging data, the fractures were predominantly medium- to high-angle, ranging from 40° to 70°, and oriented in the NW-SE direction, which was generally consistent with the fault strike. Figure 3 shows a stereo plot of the fractures interpreted in the fractured granite reservoir.

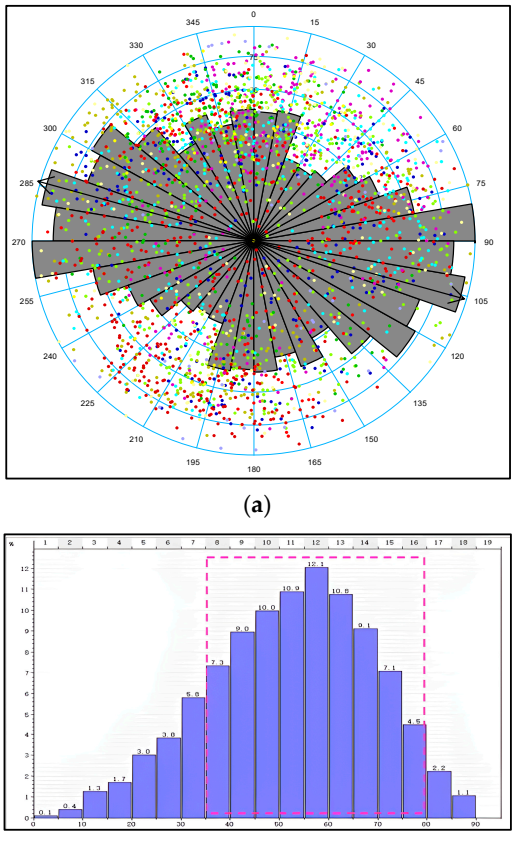

(**a**)

(**b**)

Figure 3. (**a**) Dominant fracture orientations in the NW-SE direction. (**b**) Dominant fracture with medium to high dip angles (40°–70°).

Furthermore, based on drilling, logging, and seismic data and guided by the theory of fault closure, a study of the sealing capacity was conducted through qualitative and quantitative evaluations of the faults and cap rocks. This study, which built upon the stratigraphic correlation, structural interpretation, and reservoir property predictions, provided a basis for assessing the feasibility of gas injection development in the fractured basement complex reservoir. Geological research indicated that the boundary faults had a good sealing capacity, while the intra-block faults exhibited a poor sealing capacity, which did not affect gas injection development.

The 3D geological model is a three-dimensional visualization of the reservoir characterization results. It integrates multidisciplinary data to enable a quantitative 3D description and prediction of the geological features. A detailed 3D geological model was developed, resulting in a variable-depth corner-point grid system. A permeability model of the sandstone reservoir is shown in Figure 4. After coarsening, the planar grid size was 50 m × 50 m; the vertical grid thickness was 1 m for sandstone and 5 m for the basement. The block size of the fractured basement complex reservoir was 50 m × 50 m × 1 m, and DX-DY-DZ was 85 × 57 × 253 in the matrix and fracture grid.

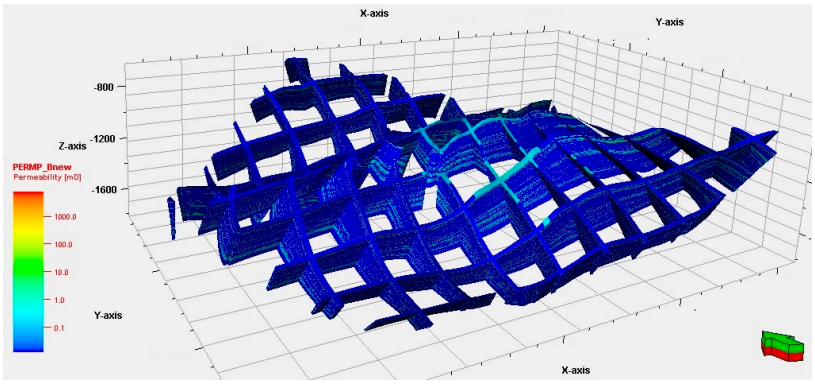

Figure 4. Permeability model of the sandstone reservoir.

The DFN (discrete fracture network) model integrates data from geophysics, geology, and reservoir engineering, enabling a systematic description of the fractures. Based on the fracture characterization, the orientations and dip angles of the fractures interpreted from borehole imaging (BHI) logging were analyzed. The dominant fracture orientations in the area were in the NW and NE directions, with medium to high dip angles (40° to 70°).

A statistical analysis of the correlation between the fracture intensity and seismic attributes indicates a strong correlation with ant-tracking and maximum likelihood attributes. These attributes were therefore used as the constraints to conduct two sets of stochastic simulations of the fracture distribution, resulting in a spatial distribution model of the fracture networks. Using seismic attribute constraints, two sets (NW and NE) of stochastic simulations of the fracture distribution were conducted, resulting in a spatial distribution model of the fracture networks. A DFN model of the fractured basement complex reservoir is shown in Figure 5.

2.2.2. The Building Reservoir Simulation Model

To analyze the nitrogen gas injection performance in the fractured basement complex reservoir, a 3D reservoir model with complex natural fractures was built in a numerical reservoir simulator. The numerical simulation of the fractured basement complex reservoir differed significantly from the traditional single-porosity, single-permeability or dual-porosity, dual-permeability models. Special methods were required for the geological modeling and reservoir simulation, with the specific principles outlined as follows:

(1) The geological model was vertically divided into N layers, which were defined as 2N layers in the numerical simulation. This meant the model contained two systems: sandstone (matrix) and the fractures.
(2) The sandstone (matrix) block model was assigned reservoir properties such as permeability and porosity, with the grid block size corresponding to the simulation grid size.
(3) The fracture model was assigned natural fracture properties, including fracture permeability and porosity.
(4) The interporosity flow coefficient represented the ease of fluid exchange between the fracture system and the matrix block system in the dual-porosity reservoir.

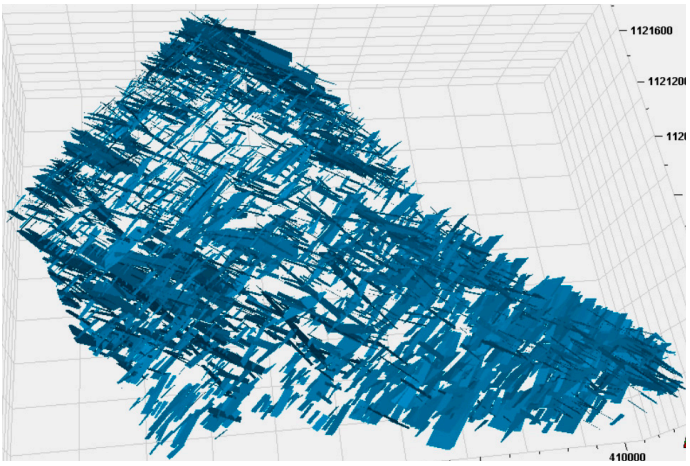

Figure 5. DFN model of the fractured basement complex reservoir.

A schematic diagram of the principles of the dual-media simulation is shown in the Figure 6. This approach allowed for the implementation of both dual-porosity, dual-permeability and dual-porosity, single-permeability models.

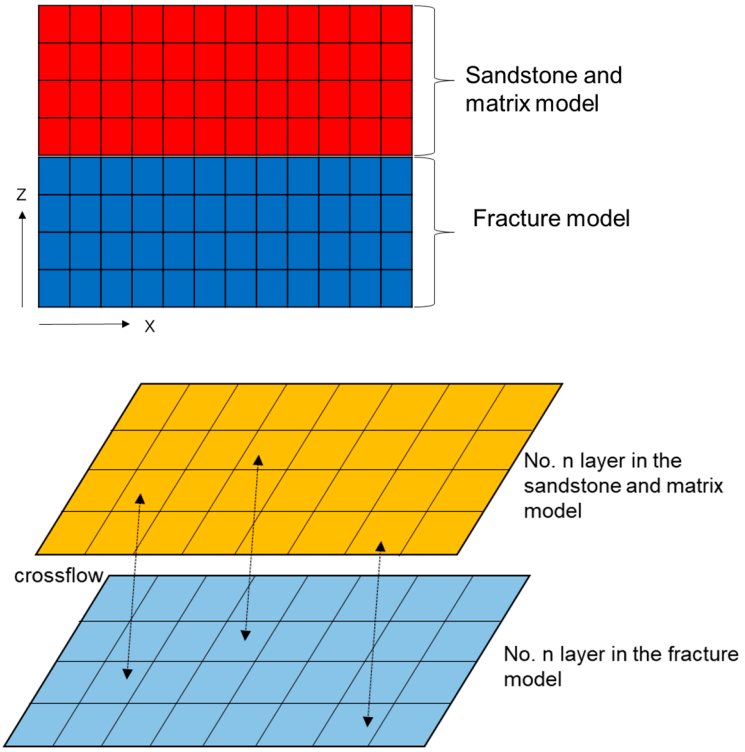

Figure 6. Schematic diagram illustrating the dual-medium simulation approach used in this study.

Different control properties were set for each reservoir and region to establish a single-medium numerical model for the sandstone reservoirs. The fracture properties corresponding to the sandstone reservoir were assigned a value of 0, the sandstone block factor was set to 0, and the fracture system was deactivated.

The geological modeling incorporated 3D seismic interpretation and borehole imaging to construct a discrete fracture network (DFN) model representing the fracture geometry, density, and connectivity. The fracture permeability and porosity were calibrated using well testing data, while the matrix properties were derived from a core analysis. This model was integrated into a dual-porosity framework for simulating the fluid flow between the fractures and the matrix, as well as in the fractured basement reservoir and the sandstone reservoir.

The simulation approach demonstrated high adaptability, as the dual-porosity and DFN models were transferable to other reservoirs with similar fracture characteristics. This study provides a practical framework for enhancing the oil recovery in diverse fractured reservoir settings, ensuring scalability and customization.

2.2.3. Simulation Parameters

After upscaling the model using software, porosity and permeability models for the fractures were generated. The fracture conductivity was 30.5 mD·m from the well testing data. The relative permeability curve and the other parameters were obtained from the relative permeability experiments above. The reservoir and fracture properties used in the simulation are summarized in Table 5.

Table 5. Basic reservoir and fracture properties used for fractured reservoir simulations.

Parameter	Value
Number of grid blocks (DX × DY × DZ)	85 × 57× 253 (2 set)
Block size (x × y × z)	50 m × 50 m × 1 m
Reservoir temperature	92.4 °C
Reservoir permeability	8 mD
Matrix porosity	6%
Rock compressibility	14.5×10^{-4} MPa^{-1}
Initial formation pressure	15.0 MPa
Reservoir mid-depth	1354.7 m
Reservoir GOR	19.0 m^3/m^3
Oil viscosity	2.55 mPa·s
K_v/K_H	0.10
Well radius	0.15 m
Fracture length	50–400 m
Dip angle	40°–70°
Fracture conductivity	30.5 mD·m

2.2.4. History Matching

The fractured basement complex reservoir was developed using an irregular well pattern with water injection. There were 29 wells, including 24 oil producers and 5 water injectors. The complex reservoir was in a gradual decline phase at the time. After the injection of water into the sandstone, the formation pressure significantly increased, but the pressure maintenance was still below 50%. It was necessary to study effective methods for reasonable energy supplementation. Based on the laboratory tests and the model built using the novel method, gas injection was optimized in the fractured basement complex reservoir.

History matching was conducted by comparing the simulated production performance with actual field data, including the pressure trends, oil recovery rates, and gas–oil ratio. The model parameters, such as the permeability, porosity, and fracture properties, were iteratively adjusted until the simulated results matched the field data within acceptable

error limits. The relative errors were minimized to 3.4% for cumulative oil production and 4.2% for cumulative liquid production. The single-well matching accuracy reached approximately 90%, demonstrating the model's reliability for predictive simulations.

To validate the accuracy of the simulation framework, sensitivity tests were performed on key reservoir parameters, including fracture permeability and conductivity. These tests confirmed that variations within ±10% of the base values resulted in a less than 5% deviation in the recovery predictions, underscoring the robustness of the simulation approach.

Simultaneously, the process generated distributions for the remaining oil and pressure, providing initialization conditions for optimizing development plans. The forecast simulation time was about 20 years.

3. Results Analysis

3.1. Laboratory Results

3.1.1. The MMP Testing Results

Slim-tube displacement experiments were conducted at different pressures to evaluate the degree of miscibility. The results indicated that when CO_2 was injected at a pressure of 12.23 MPa and an injection volume of 1.2 PV, the oil recovery efficiency exceeded 90%. Therefore, this pressure could be considered the MMP. Using this method, the MMPs of the other three kinds of gases (APG, oxygen-reduced air, and N_2) were researched, which are shown in Table 6.

Table 6. Summary of MMPs for different gas.

Gas Type	MMP (MPa)
CO_2	12.23
APG	17.15
Air	83.61
N_2	107.85

Under the current reservoir pressure and temperature conditions, none of the injected gases could achieve miscibility, and the oil recovery primarily relied on gas cap gravity drainage.

3.1.2. The Core Flooding Efficiency

The displacement efficiency for these four different gases is summarized in Table 7. Four kinds of gases were used in long-core gas flooding efficiency experiments, and all of the results are shown in Figure 7. CO_2 had the highest oil recovery efficiency, reaching 74.97%. This was because under the experimental conditions, CO_2 achieved miscible pressure with the crude oil, forming a miscible phase that enhanced the oil recovery efficiency. APG had the second highest recovery efficiency, reaching 59.59%. It contained a certain proportion of light hydrocarbon components that could partially dissolve in the crude oil, improving its flow ability. Air had an oil recovery efficiency of 54.16%. It contained a small amount of oxygen, which could promote slight oxidation of the crude oil, though thus effect was limited. N_2 had the lowest oil recovery efficiency, at only 51.64%. N_2 did not dissolve in the crude oil and relied mainly on physical displacement, resulting in a relatively lower efficiency.

The experimental studies showed that CO_2 had the highest oil recovery efficiency, primarily because its low miscible pressure allowed it to achieve a miscible state under the experimental conditions, significantly enhancing the recovery efficiency. The other three gases (APG, oxygen-reduced air, and N_2) exhibited similar oil recovery efficiencies in a

non-miscible state, mainly influenced by their physical properties and interactions with the crude oil.

Table 7. Summary of displacement efficiency for different gases.

Gas Type	Kair (mD)	Porosity (%)	Oil Saturation (%)	Injection Rate (cm^3/min)	Displacement Efficiency (%)
CO_2	1.68	13.63	60.4	0.01	70.3
APG	0.94	12.58	59.0	0.01	64.5
Air	1.28	11.01	58.2	0.01	53.5
N_2	2.25	14.40	61.5	0.01	50.5

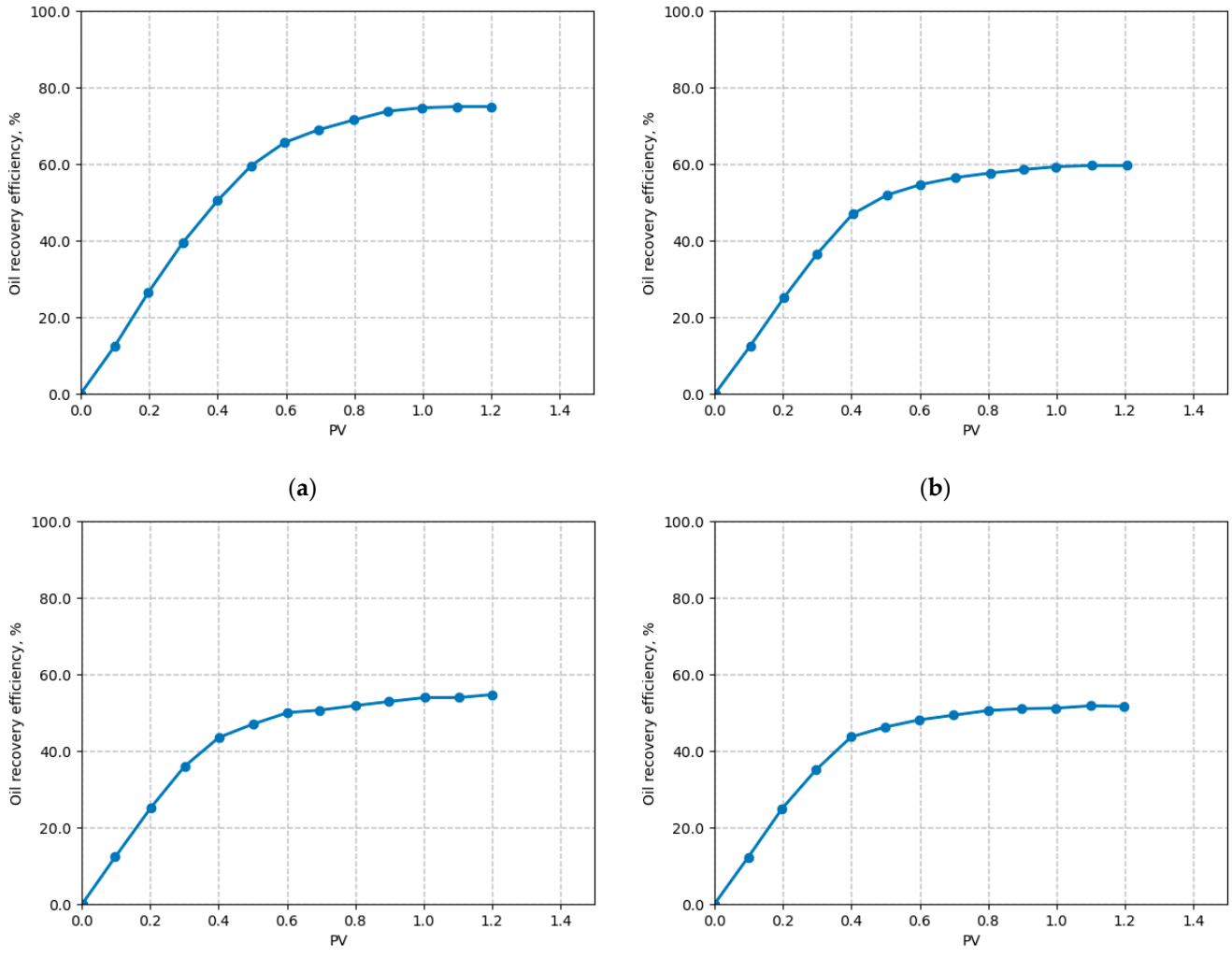

Figure 7. Oil recovery efficiencies of four gases (CO_2, APG, air, and N_2) from core flooding experiments. (**a**) Oil recovery efficiency for CO_2 gas flooding. (**b**) Oil recovery efficiency for APG gas flooding. (**c**) Oil recovery efficiency for air gas flooding. (**d**) Oil recovery efficiency for N_2 gas flooding.

According to the MMP tests and the long-core flooding experiments, CO_2 only exhibited significant advantages under miscible conditions. However, injecting CO_2 imposed considerable burdens on the wellbores and the gathering and transportation systems. Compared to APG injection, N_2 was easy to obtain, cost-effective, and safe to inject. So, implementing nitrogen injection in developing the fractured basement complex reservoir was recommended.

3.1.3. Relative Permeability Analysis

The movable oil saturation range during gas flooding in the matrix was 40.3% to 61%, with a residual oil saturation of 39%. This indicated that approximately 40.3% to 61% of the crude oil could be displaced during matrix gas flooding, while the remaining 39% remained trapped in the formation. The oil recovery efficiency in the matrix core was 37.4%. For gas flooding in the fractures, the movable oil saturation range was 35% to 70%, with a residual oil saturation of 29.7%. This meant that about 35% to 70% of the crude oil could be displaced during fracture gas flooding, while 29.7% of the oil remained in the formation. The efficiency of gas flooding in the cores with artificial fractures was about 52.7%. Using the same method, gas flooding experiments were conducted on sandstone. The movable oil saturation range during sandstone gas flooding was 35% to 64%, with a residual oil saturation of 36%. This indicated that approximately 35% to 64% of the crude oil could be displaced during the gas flooding process, while the remaining 36% stayed trapped in the formation.

Gas flooding in the sandstone, the matrix, and the fractured matrix exhibited different performances in terms of the movable oil saturation range and the residual oil saturation, which are shown in Figures 8 and 9. Among these, the gas flooding in the fractured matrix achieved the best results, with the widest movable oil saturation range and the lowest residual oil saturation, making it an effective method for enhancing the reservoir recovery. The gas flooding in the matrix was second, while the gas flooding in the sandstone showed a lower efficiency. Gas injection for oil recovery in a fractured basement complex oil reservoir could be utilized to achieve the optimal development performance.

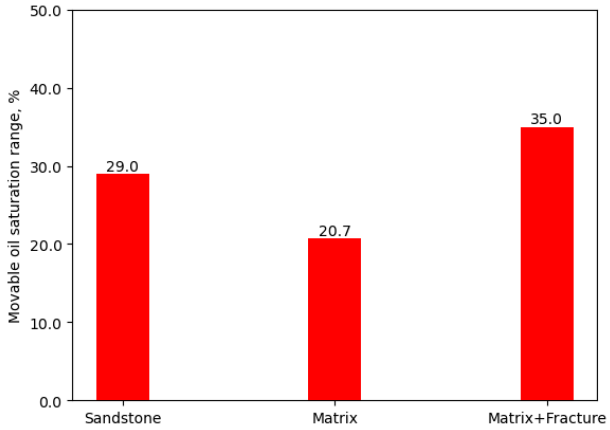

Figure 8. Movable oil saturation range in three different media (sandstone, matrix, and fractured matrix) after gas flooding.

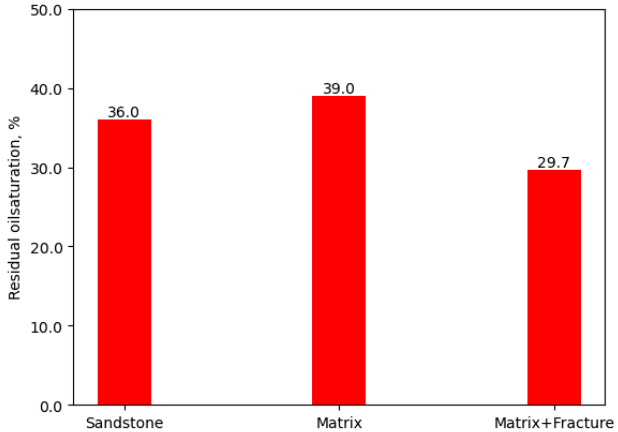

Figure 9. Residual oil saturation in 3 different media (sandstone, matrix, and fractured matrix) after gas flooding.

From the experimental mechanism studied above, the residual oil saturation for sandstone after water flooding was 23.7%, while for gas flooding, it was 36%. Gas flooding resulted in an even lower residual oil saturation in the fracture system and was more suitable for the fractured basement reservoir. High-permeability sandstone showed a greater advantage with water flooding compared to gas flooding.

3.2. Simulation Results

3.2.1. The Optimal Injection Rate

Based on the liquid production rate of the fractured basement complex reservoir, four gas injection cases were designed with daily injection rates of 30,000 m^3/d, 50,000 m^3/d, 70,000 m^3/d, and 90,000 m^3/d, and the oil recovery in these case is shown in Figure 10. By analyzing the oil increment effects in each case, the optimal gas injection rate was recommended. According to the data from the reservoir numerical simulation, a daily gas injection rate of 50,000 m^3/d achieved a moderate increase in the reservoir pressure, effectively improved the crude oil's mobility, and delivered the best oil recovery performance. When the gas injection rate exceeded 50,000 m^3/d, the increase in the reservoir pressure diminished, and the incremental oil recovery effect no longer improved significantly. Excessive gas injection not only raised the operational costs but also increased the risk of gas channeling.

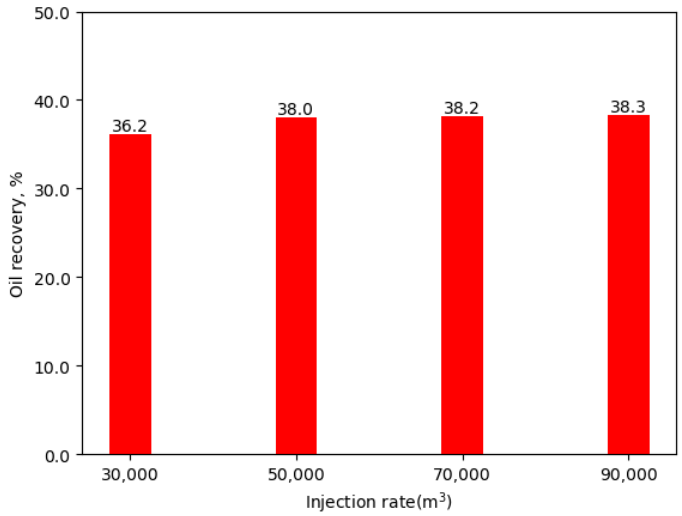

Figure 10. Comparison of oil recovery with 4 different gas injection rates.

Implementing nitrogen injection at a rate of 50,000 m^3/day did pose logistical challenges, particularly regarding the operational costs and gas availability. An onsite nitrogen generator was used to alleviate the supply constraints in the research area, and high-capacity compressors and infrastructure were required to maintain the injection rate, but these would require additional equipment investments. These challenges underscore the importance of a detailed feasibility study to optimize the balance between cost, supply reliability, and project economics.

3.2.2. The Cyclic Injection Strategy

Cyclic gas injection is an important technical approach to enhancing oil recovery. By scheduling the injection and shut-in periods, gas channeling could be effectively controlled, leading to increased oil recovery. Six cyclic gas injection cases were designed: injecting for 1 month and shutting in for 11 months, injecting for 2 months and shutting in for 10 months, injecting for 3 months and shutting in for 9 months, injecting for 6 months and shutting

in for 6 months, injecting for 8 months and shutting in for 4 months, and injecting for 10 months and shutting in for 2 months.

The results of the reservoir numerical simulation are shown in Table 8 and Figure 11. It was seen that cyclic gas injection caused significant production fluctuations. While the daily oil production initially increased compared to that with continuous injection, it quickly declined. This reflected that gas channeling was partially suppressed, and it also indicated an insufficient fluid supply due to a decline in reservoir pressure.

Table 8. Statistics of cyclic gas injection strategies.

Mode	Cumulative Gas Injection Volume ($\times 10^8$ m^3)	Cumulative Gas Production Volume ($\times 10^8$ m^3)	Gas Left in the Reservoir ($\times 10^8$ m^3)	Oil Recovery (%)
Inject for 1 M, shut for 11 M	0.255	0.069	0.186	37.24
Inject for 2 M, shut for 10 M	0.510	0.313	0.197	37.39
Inject for 3 M, shut for 9 M	0.765	0.557	0.208	37.53
Inject for 6 M, shut for 6 M	1.472	1.236	0.236	37.76
Inject for 8 M, shut for 4 M	1.960	1.703	0.257	37.88
Inject for 10 M, shut for 2 M	2.463	2.204	0.259	37.94
Continuous injection	3.059	2.797	0.262	38.00

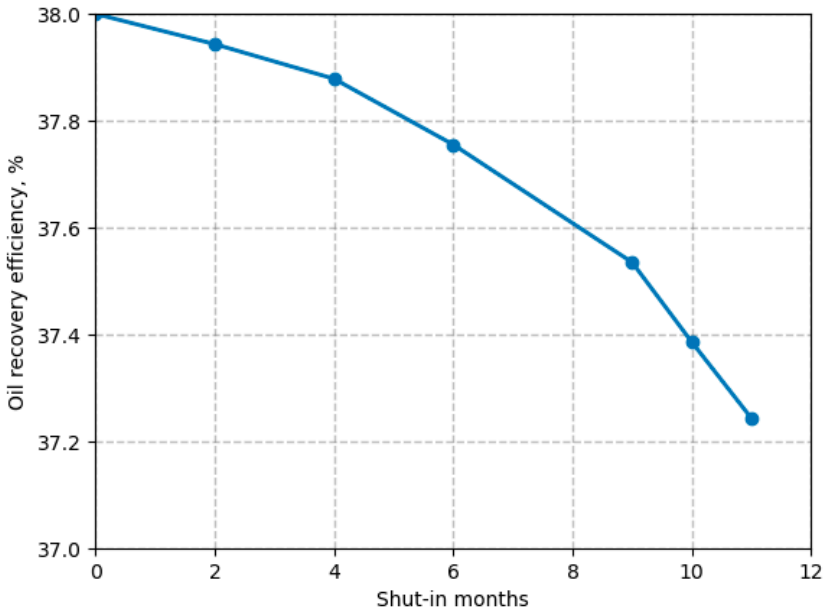

Figure 11. Oil recovery performance for six cyclic gas injection scenarios, varying the injection and shut-in periods.

Overall, the larger the cumulative gas injection, the higher the cumulative oil production. However, as the gas volume left in the reservoir reached a certain threshold, the increment began to slow down. According to the results of optimization of the numerical simulation, lower injection cycles led to a lower cumulative oil production. When the injection cycle dropped below 67%, the cumulative oil production declined more rapidly, and when it fell below 25%, this decline became steep. Therefore, the recommended development approach was to inject gas for 8 months and shut in for 4 months.

3.2.3. Gas Injection Location

Three cases were designed: no gas injection development, gas injection in the middle of the fractured basemen complex reservoir, and gas injection at the top. The oil recovery in these cases was 28.6%, 34.1%, and 38.0%, respectively, as shown in Figure 12. The

numerical simulation results indicated that the gas injection at the top of the fractured basement complex reservoir showed a significantly better oil recovery compared to that with the gas injection in the middle and no gas injection development. Gas injected at the higher structures formed a larger artificial gas cap volume than the gas injection in the middle, providing better pressure maintenance and a superior development performance.

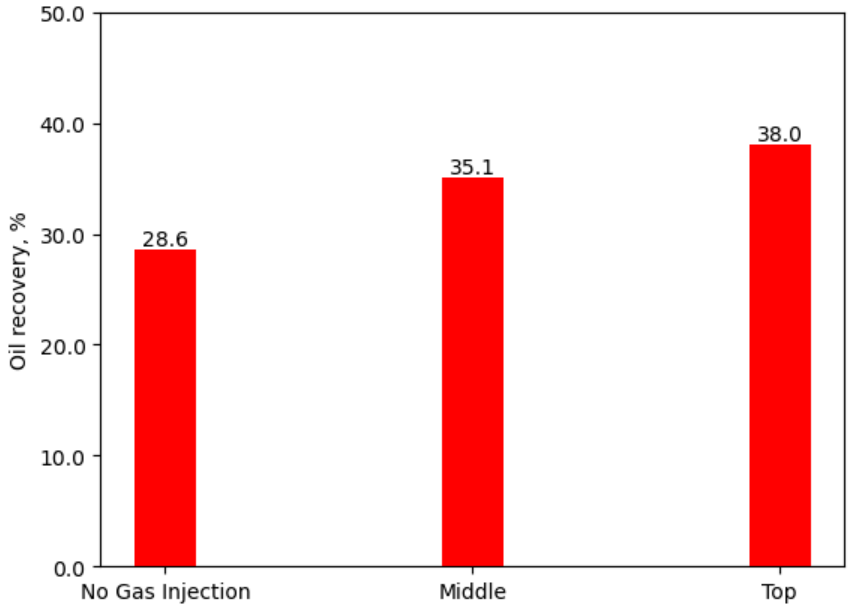

Figure 12. Comparison of oil recovery under three development scenarios (no gas injection development, gas injection in the middle, and gas injection at the top).

4. Discussions

4.1. Simulation and the Geological Impact

This combined experimental and modeling workflow is applicable to a wide range of fractured reservoirs, but the recovery factor in gas injection is sensitive to geological variations. The impact of geological variations was evaluated by modifying the reservoir characteristics in the simulation models. For instance, a transition from fractured granite to a carbonate lithology can introduce additional mechanisms, such as matrix dissolution, which may improve the recovery efficiency for miscible injection but limit the effectiveness of immiscible nitrogen injection. Conversely, lower-permeability rocks, such as dense metamorphic formations, would reduce the fracture connectivity, increasing gas channeling risks and requiring higher injection pressures.

To quantify these effects, sensitivity analyses were performed by varying the porosity ($\pm$20%), permeability ($\pm$30%), and fracture intensity ($\pm$25%). The results indicated that the oil recovery decreased by up to 15% when the permeability and fracture intensity were reduced, while a higher porosity and fracture density increased the recovery by approximately 10% due to the enhanced sweep efficiency. These findings highlight the adaptability of the proposed nitrogen injection strategy, although the optimal parameters should be recalibrated for reservoirs with significantly different geological characteristics.

4.2. A Comparative Analysis

Previous studies on fractured basement reservoirs have predominantly focused on CO_2 and other miscible gas injection techniques, emphasizing their ability to achieve miscibility and enhance the oil displacement efficiency. In contrast, this study demonstrated the viability of nitrogen injection under immiscible conditions, achieving substantial oil recovery through gravity-assisted drainage and optimizing the gas utilization. Unlike

previous works, our findings revealed that immiscible nitrogen injection, when applied with cyclic strategies, mitigated gas channeling while leveraging the natural fracture networks to improve the recovery efficiency.

This study provides novel insights into nitrogen injection and its application in fractured basement complex reservoirs. The laboratory experiments show that nitrogen injection achieves a wide movable oil saturation range (35–70%) in fractured matrices, with a residual oil saturation as low as 29.7%, despite its immiscible nature. Furthermore, the optimized cyclic injection strategy—8 months of injection followed by a 4-month shut-in period—yields a recovery factor of 37.9%, balancing an incremental recovery with minimized gas channeling risks. This cyclic approach leverages the pressure redistribution during shut-in periods to enhance the sweep efficiency.

The development strategy for the fractured basement complex reservoir involved the injection of water into the sandstone combined with the injection of gas into the fractured basement reservoir. Gas was injected at the top of the complex reservoir, with an optimal injection rate of 50,000 m^3/d. A cyclic gas injection approach was adopted, injecting gas for 8 months, followed by a 4-month shut-in period. This combined water injection and gas injection strategy achieved a recovery factor of nearly 40%, demonstrating a significant development efficiency.

4.3. Limitations and Future Work

While this study primarily focused on technical optimization, future evaluations should incorporate an economic analysis to validate the recommended strategies. Key factors include the capital costs, operational costs, economic returns, and risk factors. Our preliminary estimates suggested that the benefits of enhanced recovery using cyclic injection outweighed the costs, but a detailed economic model needs to be built in future research.

5. Conclusions

This study demonstrates the viability and optimization of nitrogen gas injection for enhanced oil recovery in fractured basement complex reservoirs through integrated laboratory experiments and numerical simulations. The laboratory results revealed that nitrogen injection, despite being immiscible, achieved a recovery efficiency of 51.64% with the widest movable oil saturation range (35–70%) and the lowest residual oil saturation (29.7%) among the gases tested, establishing it as a cost-effective alternative to CO_2 under low-pressure conditions. Through the numerical simulation, an optimized cyclic injection strategy consisting of an 8-month injection period followed by a 4-month shut-in period was identified, yielding a recovery factor of 37.9% while effectively minimizing gas channeling risks. This study further established that the injection location significantly impacts the recovery performance, with injection at the top into high-structure fractures achieving the highest recovery factor of 38.0%, compared to 34.1% for injections in the middle and 28.6% for no injection. Additionally, an optimal daily nitrogen injection rate of 50,000 m^3/d was determined to balance the recovery performance with operational feasibility. These findings provide practical guidelines for implementing nitrogen injection in fractured basement complex reservoirs, demonstrating that proper optimization of the injection parameters, particularly the cycle timing and injection location, can significantly enhance the oil recovery while managing the operational challenges inherent to fractured basement complex reservoirs.

Author Contributions: Conceptualization, Y.J.; methodology, F.X. and J.O.; software, F.X. and S.L.; result analysis, J.O. and F.X.; investigation, J.Z. and F.X.; discussion, X.G. and F.X.; data collection,

S.L. and D.L.; writing, F.X. and J.O. All authors have read and agreed to the published version of the manuscript.

Funding: This research received no external funding.

Data Availability Statement: The data used in this research are confidential.

Acknowledgments: The authors would like to acknowledge the support from all of the researchers related to this research.

Conflicts of Interest: Authors Ying Jia, Jingqi Ouyang, Feng Xu and Juntao Zhang were employed by the company CNPC. Author Xiaocheng Gao, Shiliang Liu and Da Li was employed by the company PetroChina. The remaining authors declare that the research was conducted in the absence of any commercial or financial relationships that could be construed as a potential conflict of interest. The CNPC had no role in the design of the study; in the collection, analyses, or interpretation of data; in the writing of the manuscript, or in the decision to publish the results.

References

1. May, J.; Hewitt, R. The Nature of the Basement Complex Oil Reservoir, Edison Oil Field, California. *AAPG Bull.* **1947**, *31*, 2239–2240.
2. Mancini, E.; Mink, R.; Tew, B.; Bearden, B. Natural gas plays in Jurassic reservoirs of southwestern Alabama and the Florida panhandle area. *AAPG Bull.* **1990**, *40*, 513–519.
3. Mancini, E.; Mink, R.; Tew, B.; Kopaska-Merkel, D.; Mann, S. Upper Jurassic smackover oil plays in Alabama, Mississippi and the Florida Panhandle. *Gulf Coast Assoc. Geol. Soc. Trans.* **1991**, *41*, 475–480.
4. Wilson, T.; Zheng, L.; Shumaker, R. Sequential development of structural heterogeneity in the Granny Creek oil field of West Virginia. *AAPG Bull.* **1993**, *77*, 8.
5. Mink, R.; Mancini, E. Lower Cretaceous and Upper Jurassic oil reservoirs of the updip basement structure play: Southwest Alabama. *AAPG Bull.* **1995**, *79*, 10.
6. Kireev, F.; Dong, T.; Tuan, P. Composition, Structure and Oil-Bearing Capacity of the Basement in the White Tiger Field. In Proceedings of the Indonesian Petroleum Association 26th Annual Convention, Jakarta, Indonesia, 18–20 May 1998.
7. Malim, E.; Daungkaew, S.; Hansen, S.; Oo, A.; Hussain, R.; Kurniawan, S.; Zulkefli, Z. Integrated Fracture Evaluation of a Malaysian Basement Well Drilled with the Oil-Based Mud. In Proceedings of the Petroleum Geology Conference and Exhibition, Kuala Lumpur, Malaysia, 14–15 January 2008.
8. McGeer, A.; Refani, M. Dynamically Conditioned Modeling to Address Development Challenges in a Highly Complex Fractured Basement Reservoir, Yemen. In Proceedings of the SPE Reservoir Characterisation and Simulation Conference and Exhibition, Abu Dhabi, United Arab Emirates, 17–19 September 2019.
9. Kharrat, R.; Ott, H. A Comprehensive Review of Fracture Characterization and Its Impact on Oil Production in Naturally Fractured Reservoirs. *Energies* **2023**, *16*, 3437. [CrossRef]
10. Amerighasrodashti, A. Immiscible and Miscible Gas-Oil Gravity Drainage in Naturally Fractured Reservoirs. Ph.D. Thesis, Delft University of Technology, Delft, The Netherlands, 2014.
11. Dinh, H.; Le, N.; Peter, M.; Nguyen, V.; Dang, T.; Nguyen, V.; Hoang, N.; Truong, T.; Tran, H.; Nguyen, K. Gas-assisted gravity drainage GAGD Huff n puff application for fractured basement reservoir-Case study. In Proceedings of the SPE Asia Pacific Oil and Gas Conference and Exhibition, Jakarta, Indonesia, 17–19 October 2017.
12. Ma, M.; Emami-Meybodi, H. Multiscale non-equilibrium compositional modeling of cyclic gas injection in shale reservoirs. In Proceedings of the SPE Annual Technical Conference and Exhibition, New Orleans, LA, USA, 23–25 September 2024.
13. Zhao, L.; Zhang, L.; Su, Y.; Tan, X.; Li, C.; Wang, S. In-situ CT study on the effect of cyclic gas injection and depletion exploitation on the phase behavior of fractured condensate gas reservoirs. *Front. Earth Sci.* **2024**, *12*, 1418821. [CrossRef]
14. Xie, J.; Neima, A. Cyclic gas injection EOR pilot in tight Viking sand pool. In Proceedings of the SPE Improved Oil Recovery Conference, Tulsa, OK, USA, 22–25 April 2024.
15. Enab, K. Impact of diffusion and adsorption on the performance of CO_2, CH_4, and cyclic gas huff-n-puff injection into light oil reservoirs. In Proceedings of the Abu Dhabi International Petroleum Exhibition and Conference, Abu Dhabi, United Arab Emirates, 2–5 October 2023.
16. Ghanizadeh, A.; Song, C.; Cesar, J.; Jiang, C. Evaluation of produced hydrocarbons composition during cyclic CO_2 injection (huff-n-puff) in artificially-fractured shale core sample. In Proceedings of the SPE Canadian Energy Technology Conference, Calgary, AB, Canada, 15–16 March 2023.

17. Youssif, M.I.; Sharma, K.; Piri, M. Hydrocarbon gas foam injection in fractured oil-wet carbonate samples: An experimental investigation of the effect of fracture-matrix permeability contrast on oil recovery. In Proceedings of the SPE Canadian Energy Technology Conference, Calgary, AB, Canada, 15–16 March 2023.
18. Alimohammadi, N.; Pooladi-Darvish, M.; Rostami, B.; Khosravi, M. Improvement to gravity drainage recovery by repressurization as a criterion to screen and rank naturally fractured reservoirs for gas injection. *SPE Reserv. Eval. Eng.* **2022**, *26*, 1073–1090. [CrossRef]
19. Gugl, R.; Kharrat, R.; Shariat, A.; Ott, H. Evaluation of gas-based EOR methods in gas-invaded zones of fractured carbonate reservoirs. *Energies* **2022**, *15*, 4921. [CrossRef]
20. Wei, F.; Zhang, S.; Xi, Y.; Zhu, Z.; Xiong, C.; Zang, C.; Li, J. Conformance control for tight oil cyclic gas injection using foam. *Geofluids* **2022**, *2022*, 6571525. [CrossRef]
21. Bueno Zapata, N.; Mejía Cárdenas, J.M.; Martínez Paternina, J.J. Flue gas and nitrogen co-injection during cyclic steam stimulation in heavy oil reservoirs: A numerical evaluation. *Dyna* **2021**, *88*, 143–153. [CrossRef]
22. Sennaoui, B.; Pu, H.; Malki, M.L.; Afari, A.S.; Larbi, A.; Tomowewo, O.S.; Araghi, R.H.R. Laboratory experiments on the cyclic gas injection process using CO_2, C_2H_6, and C_3H_8 to evaluate oil recovery performance and mechanisms in unconventional reservoirs. In Proceedings of the ARMA/DGS/SEG International Geomechanics Symposium, Abu Dhabi, United Arab Emirates, 7–10 November 2022.
23. Song, Z.; Li, M.; Zhao, C.; Yang, Y.-L.; Hou, J. Gas injection for enhanced oil recovery in two-dimensional geology-based physical model of Tahe fractured-vuggy carbonate reservoirs: Karst fault system. *Pet. Sci.* **2020**, *17*, 419–433. [CrossRef]
24. Sahai, R.; Moghanloo, R. Impact of stimulated reservoir volume in the efficacy of miscible gas injection EOR in shale reservoirs. In Proceedings of the SPE Improved Oil Recovery Conference, Virtual, 25–29 April 2022.
25. Safaei, A.; Kazemzadeh, Y.; Riazi, M. Mini review of miscible condition evaluation and experimental methods of gas miscible injection in conventional and fractured reservoirs. *Energy Fuels* **2021**, *35*, 7064–7075. [CrossRef]
26. Augustine, C.; Johnston, H.E.; Young, D.; Amini, K.; Uzun, I.; Kazemi, H. Evaluation of energy storage potential of unconventional shale reservoirs using numerical simulation of cyclic gas injection. *J. Energy Resour. Technol.* **2021**, *143*, 112004. [CrossRef]
27. Nelson, R. *Geologic Analysis of Naturally Fractured Reservoirs*; Gulf Professional Publishing: Houston, TX, USA, 2001.
28. Narr, W.; Schechter, D.; Thompson, L. *Naturally Fractured Reservoir Characterization*; Society of Petroleum Engineers: Richardson, TX, USA, 2006.
29. Lonergan, L.; Jolly, R.; Rawnsley, K.; Sanderson, D. *Fractured Reservoirs*; Geological Society: London, UK, 2007.
30. Ray, D.; Al-Shammeli, A.; Verma, N.; Matar, S.; De Groen, V.; De Joussineau, G.; Ghilardini, L.; Le Maux, T.; Al-Khamees, W. Characterizing and Modeling Natural Fracture Networks in a Tight Carbonate Reservoir in the Middle East: A methodology. *Bull. Geol. Soc. Malays.* **2012**, *58*, 29–35.
31. Nie, Z.; Xu, F.; Ouyang, J.; Li, X.; Zhang, J.; Liu, S.; Han, J.; Li, D. Experimental tests and EDFM method to study gas injection in a fractured granite reservoir. *Front. Energy Res.* **2023**, *10*, 1008356. [CrossRef]
32. Hammam, M.; Soliman, K. Novel dual porosity simulation workflow and solutions for the 3D fracture modeling. In Proceedings of the Mediterranean Offshore Conference, Alexandria, Egypt, 20–22 October 2024.
33. Yu, X.; Kang, Z.; Li, Y.; Lin, X.; Xie, L.; Li, J. Integration of geological model and numerical simulation technique to characterize the remaining oil of fractured biogenic limestone reservoirs. *Arab. J. Sci. Eng.* **2024**, *49*, 1–17. [CrossRef]
34. Zheng, S.; Wang, X.; Chen, J.; Gu, H.; Wu, W. Multiphase flow simulation of fractured karst oil reservoirs applying three-dimensional network models. *Phys. Fluids* **2024**, *36*, 076610. [CrossRef]
35. Khoei, A.; Taghvaei, M. A computational dual-porosity approach for the coupled hydro-mechanical analysis of fractured porous media. *Int. J. Numer. Anal. Methods Geomech.* **2024**, *48*, 1745–1773. [CrossRef]
36. Chen, D.; Zhang, C.; Yang, M.; Li, H.; Wang, C.; Diwu, P.; Jiang, H.; Wang, Y. Research on water invasion law and control measures for ultradeep, fractured, and low-porosity sandstone gas reservoirs: A case study of Kelasu gas reservoirs in Tarim Basin. *Processes* **2024**, *12*, 310. [CrossRef]
37. Warren, J.; Root, P. The Behavior of Naturally Fractured Reservoirs. *SPE J.* **1963**, *3*, 245–255. [CrossRef]
38. Cinco, L.; Samaniego, V.; Dominguez, A. Transient Pressure Behavior for a Well With a Finite-Conductivity Vertical Fracture. *SPE J.* **1978**, *18*, 253–264. [CrossRef]
39. Karimi-Fard, M.; Firoozabadi, A. Numerical Simulation of Water Injection in Fractured Media Using the Discrete-Fracture Model and the Galerkin Method. *SPE Reserv. Eval. Eng.* **2003**, *6*, 117–126. [CrossRef]
40. Hoteit, H.; Firoozabadi, A. Multicomponent fluid flow by discontinuous Galerkin and mixed methods in unfractured and fractured media. *Water Resour. Res.* **2005**, *41*, 1–15. [CrossRef]

41. Zhou, W.; Banerjee, R.; Poe, B.; Spath, J.; Thambynayagam, M. Semianalytical Production Simulation of Complex Hydraulic-Fracture Networks. *SPE J.* **2013**, *19*, 06–18. [CrossRef]
42. Yuan, X.; Feng, G.; Yang, X.; Zhang, J.; Dou, S.J.; Tian, J.; Yu, G.; Zhang, K. Geological Characteristics and Production Performance of a Sandstone-Fractured Basement Composite Reservoir. In Proceedings of the International Field Exploration and Development Conference 2020 International Field Exploration and Development Conference, Chengdu, China, 23–25 September 2020.